

Single particle size and fluorescence spectra from emissions of burning materials in a tube furnace to simulate burn pits

Yong-Le Pan · Joshua D. T. Houck ·
Pamela A. Clark · Ronald G. Pinnick

Received: 19 November 2012 / Accepted: 5 March 2013 / Published online: 25 March 2013
© The Author(s) 2013. This article is published with open access at Springerlink.com

Abstract A single-particle fluorescence spectrometer (SPFS) and an aerodynamic particle sizer were used to measure the fluorescence spectra and particle size distribution from the particulate emissions of 12 different burning materials in a tube furnace to simulate open-air burning of garbage. Although the particulate emissions are likely dominated by particles $<1\ \mu\text{m}$ diameter, only the spectra of supermicron particles were measured here. The overall fluorescence spectral profiles exhibit either one or two broad bands peaked around 300–450 nm within the 280–650 nm spectral range, when the particles are illuminated with a 263-nm laser. Different burning materials have different profiles, some of them (cigarette, hair, uniform, paper, and plastics) show small changes during the burning process, and while others (beef, bread, carrot, Styrofoam, and wood) show big variations, which initially exhibit a single UV peak (around 310–340 nm) and a long shoulder in visible, and then gradually evolve into a bimodal spectrum with another visible peak (around 430–450 nm) having increasing intensity during the burning process. These spectral profiles could mainly derive from polycyclic aromatic hydrocarbons with the combinations of tyrosine-like, tryptophan-like, and other humic-like substances. About 68 % of these single-particle fluorescence spectra can be grouped into 10 clustered spectral templates that are derived from the spectra of millions of atmospheric aerosol particles observed in three locations; while the others, particularly these bimodal spectra, do not fall into any of the 10 templates. Therefore, the spectra from particulate emissions of burning materials can be easily discriminated from that of common atmospheric

aerosol particles. The SPFS technology could be a good tool for monitoring burning pit emissions and possibly for distinguishing them from atmospheric aerosol particles.

1 Introduction

Open-air burn pits are widely used for disposal of garbage, military waste, and human waste on US military bases in Iraq and Afghanistan. This practice has attracted much attention since hundreds war veterans claimed that they are suffering respiratory problems and believe that burn pit exposure is the major cause for their illnesses [1–3]. Efforts have been taken to mitigate this practice. Congress has passed legislation requiring the military to justify any further use of burn pits, and the Pentagon is conducting a review of burn pits and their current status in Iraq and Afghanistan and has shut down many in Iraq. The US Department of Defense and the Department of Veterans Affairs are proceeding cautiously in linking soldiers' symptoms to the burn pits. The Institute of Medicine, National Academy of Science, and other research institutes are conducting large-scale studies. The US Army Center for Health Promotion and Preventive Medicine (US-ACHPPM), the US Air Force Institute for Operational Health, and the US Army Research Laboratory are conducting ambient-air sampling and screening health-risk assessments [3–8]. Recently, the Institute of Medicine reported that there is no evidence linking exposure to burn pits in Iraq and Afghanistan for long-term health problems [4, 5]. The investigation from a team of doctors found that burn pit exposure within 3–5 miles was not associated with respiratory outcomes after statistical adjustment. However, increased symptom reporting was observed among Air Force deployers located within 2 miles of Joint Base Balad,

Y.-L. Pan (✉) · J. D. T. Houck · P. A. Clark · R. G. Pinnick
U.S. Army Research Laboratory, Adelphi, MD 20783, USA
e-mail: yongle.pan.civ@mail.mil

which was marginally significant with no evidence of trend [7]. Another team of doctors found that diffuse constrictive bronchiolitis might be associated with inhalational exposure in 38 soldiers [8].

Many chemicals that may present a health risk to service members were detected in the DoD air sampling from Joint Base Balad, Iraq, and Camp Lemonier, Djibouti. These samples include (a) particulate matter (PM), (b) polycyclic aromatic hydrocarbons (PAHs), (c) volatile organic compounds (VOC), and (d) toxic organic halogenated dioxins and furans (TOHDF) [9]. Exposure to chemical toxins could affect the skin, eyes, respiration, kidneys, liver, nervous system, and cardiovascular system [10–13]. Long-duration inhalation of heavy PM emissions from natural and man-made sources can cause serious heart and lung health problems [9–13]. Fortunately, most of the eye irritation, coughing and throat irritation, breathing difficulties, and skin itching are temporary for limited exposure to the burn pit emissions [10]. It is very difficult to determine, at the present stage, how exposure to burn pit affects health with given limited scientific studies and the multitude of variables, such as the variety of burning materials, burning condition, emitted particle size and concentration, the duration of exposures, near-surface wind fields, the closeness of service members to the pit, and various human factors including age, health status, existing medical conditions, and genetics [9, 10]. Further systematic and detailed studies are needed to understand the potential health effects caused by exposed to burn pit emissions. The development of a real-time monitoring system to provide service members with the information they need to reduce exposure levels near burning pits could be helpful.

Optical properties of atmospheric PM such as elastic scattering, absorption, fluorescence, and Raman spectra have been used to characterize the dynamic variability, aging process, and chemical compositions of emission from biomass burning [4–22]. Studies found that scattering and absorption efficiency strongly correlated to particle size and black carbon (BC) content related to individual fire physics [14]. Concentration of particle-related reactive oxygenated species, which is considered an important parameter in assessing the potential toxicological impact of particulate matter, could be measured by fluorescence spectra [16]. Black carbon concentrations in particulate organic matter from biomass burning can be deduced by observing pyrene fluorescence loss [17]. Fluorescence and Raman spectra are good methods for characterizing the natural carbon clusters [18]. Particle size, morphology, refractive index, carbon and PAH contents help understand the emissions [19–22]. More than 90 % of the total aerosol mass in burning emissions could be particulates of organic carbon (OC) and BC within the dominated fine aerosols (<2.5 μm) [20]. Chemical characterization

and specification of the open-air burning affluent may allow linking to potential health effects [9–13, 23–26]. The excitation-emission matrix (EEM) can identify ultra-trace amounts of particular PAHs, humic substances, dissolved organic carbon (DOC) in different complex samples [27–34], such as the determination of two of the most carcinogenic PAHs, benzo[*a*]pyrene and dibenzo[*a,h*]anthracene at a concentrations below 10 ng/L [27]. The 370-nm excited fluorescence intensity ratio between 450 and 500 nm, named as fluorescence index (FI), was found to have a significant relationship with DOC concentrations for polluted stream water [29].

Technologies based on ultra-violet laser-induced fluorescence (UV-LIF) are capable of real-time, in situ detection and classification for biological and other organic carbon aerosols (e.g., [35–38], see a review by DeFriez [39]). A single-particle fluorescence spectrometer [SPFS, ref [38] can obtain the dispersed fluorescence spectra (280–700 nm) of individual airborne aerosol particles (1–10 μm size range) as they flow through the sensor. Such a nondestructive technique has the advantage of providing near-real-time information related to the molecular compositions without requiring collection of particles, handling of the samples, or searching over a substrate for particles to be analyzed, but lacks the ability to chemically identify or specify the composition of the particle as might be possible with mass spectroscopy or other biochemical analytical methods.

In this paper, the SPFS technology is applied to measure single-particle fluorescence spectra of the particulate emissions of the controlled burning of materials. The materials were burned in a tube furnace to simulate burning from an open-air burn pit. In addition, the particle size distribution was monitored by a TSI aerodynamic particle sizer. The tube furnace was set to start at 300 °C and raised to a maximum 420 °C temperature until various test materials melted/smoldered and/or combusted. Twelve materials were selected for burning to mirror the most common garbage produced daily on military bases, such as plastics, paper, food, wood, clothing, and Styrofoam. The laboratory study described herein provides control and repeatability of burn conditions and measurements of the emission from individual burning materials, which may not be achievable in an open-air burn pit environment.

The purpose of this study is to assess the potential for monitoring particle emission from burn pits by the measurement of particle size and single-particle fluorescence spectra. Although the observed fluorescence spectral profiles are different for the various particulate emissions (excited by a 263-nm laser), but this approach falls far short of identifying PM compositions. It is even difficult to say at this early stage of research if this technology could effectively be used for monitoring particularly harmful

emissions from a burn pit, due to numerous possible molecules and many possible mixtures of molecules produced during the different burning phases, burning conditions, and aging processes. These preliminary test results reveal the fluorescence spectra and size distributions of some common burn emissions under certain burn conditions. The results suggest the UV-LIF might be a useful complementary technology for real-time in situ monitoring of burn pits to protect the service members and limit their exposure to dangerous levels of harmful burn emissions.

2 Experimental arrangement

The experimental arrangement for measuring single-particle ultra-violet laser (263 nm) induced fluorescence spectra and size of micron-sized particulate emissions from burning materials is shown in Fig. 1. The experimental setup is intended to serve as a burn pit simulator with the capability to collect UV fluorescence signatures from component materials commonly found in actual burn pits in the field (in theater). The setup has three major subsystems; a tube furnace, a single-particle fluorescence spectrometer (SPFS), and an aerodynamic particle sizer (TSI 3321).

The tube furnace was placed inside a fume hood which captures nearly all combustion products and exhausts them out of the laboratory building. The temperature of the chamber within the tube furnace (Barnstead International model F21135) can be preset to a desired temperature and automatically stabilized to that set point via a control panel and a thermocouple feedback to measure and regulate the temperature. The furnace has a 2-in. diameter bore and a ceramic tube (ID 1.75 in., OD 2.00 in., length 15 in.) that is tightly fit into the bore. Small ceramic combustion boats (length 3 in., width 1 in., depth 0.75 in.) were placed at the center of the tube to hold each test sample material. For every new material a new boat was used and inserted into the tube when the furnace temperature reached 300 °C.

Depending on the specificity of some materials, the tube furnace internal temperature was raised to a maximum at 420 °C to induce the material to melt/smolder and/or combust. A small fan, set at one end of the tube, was used to push the combustion emission particles out of the tube. The smoke PM was sampled by SPFS and TSI APS through a 1/4 in. diameter stainless steel tube at 1 L/min. The inlet of the sampling tube was set about 5 in. to the side and 10 in. above the tube end of the furnace to avoid the very high concentrations of PM coming from the tube while keeping a relatively constant particle sampling rate. All the test materials and their corresponding final furnace temperatures are listed in Table 1. The measurement for each sample took about 10–30 min depending on the time requirement to heat the material and its burn rate. For each material, thousands of single-particle UV-LIF spectra were recorded during the entire burn cycle. A fresh sample was not inserted into the tube furnace until the hood was clean and the furnace temperature again stabilized at 300 °C. The whole process was repeated three times for each material to check for repeatability.

The aerodynamic particle sizer (TSI 3321) was used to monitor the particle size distribution. The APS can measure aerodynamic size of particles in the 0.5–20 µm range independent of particle index of refraction.

The SPFS system, used here to measure the dispersed fluorescence spectra from single aerosol particles excited by a single pulse of a 263 nm UV laser, has been described previously [38]. In the measurements described in this report, a virtual impactor concentrator that would normally be placed upstream from the SPFS inlet was not needed since high enough concentrations of sampling particles were produced during the burning process. In addition, the usual 32-anode photomultiplier tube (PMT) detector for the SPFS was replaced by an image-intensified charge-coupled device (ICCD, Andor Technology, ISTAR DH734-25F-03) for better spectral resolution (~0.5 nm/pixel). Burning emissions from the tube furnace were sampled by the SPFS

Fig. 1 Experimental arrangement for measuring single-particle ultra-violet laser-induced fluorescence (UV-LIF) spectra and size of particulate emissions from various burning materials. The UV-LIF spectra are measured by a single-particle fluorescence spectrometer (SPFS). The particle size distribution is monitored by an aerodynamic particle sizer (TSI 3321)

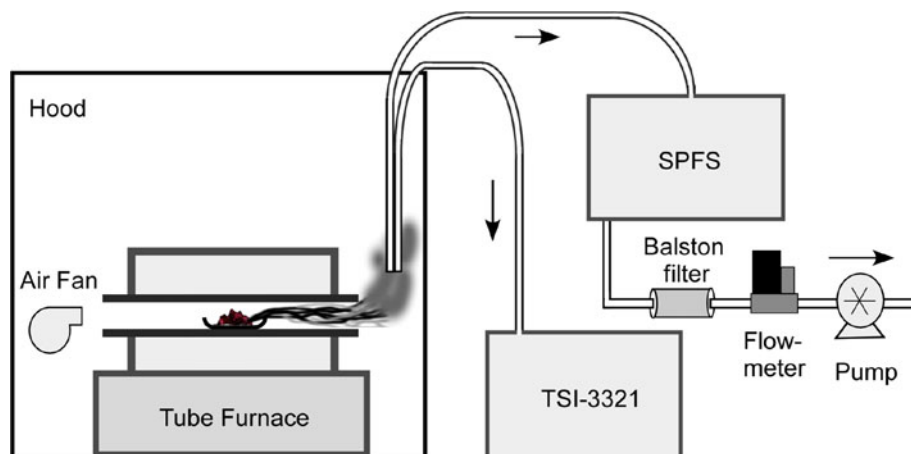


Table 1 Tested burning materials and corresponding burning temperatures

Material	Beef (cooked hamburger meat)	Bread (potato-roll bread)	Carrot (shredded carrots)	Cigarette (cut tobacco leaves)	Hair (human hair)	Uniform (battle-dress uniform)
Temperature (°C)	300–320	310–325	315–335	300–325	300–315	300–315
Material	Paper (shredded white paper)	Plastic HDPE (plastic cup)	Plastic HD (plastic spoon)	Plastic-PETE (water bottle)	Styrofoam (water cup)	Wood (2 × 4 wood shards)
Temperature (°C)	290–325	315–320	325–345	335–420	300–325	300–325

through a 1/4-in. diameter, 6-ft long stainless steel tube at 1 L/min.

The SPFS focuses the aerosol into a (about 300- μm diameter) stream using a sheath nozzle within a 2 in. cubical optical cell, which is aspirated by a piston pump (KNF Neuberger model UN 86). Particles (with size greater than about 1 μm) flowing within about 150 μm of the center of the aerosol stream are detected through their near-forward elastic scattering signals from two intersecting diode-laser beams (650 and 685 nm). A coincidence pulse from the diode beams triggers a 263-nm laser (Photonics Industries, DC-150-263, 50 μJ , 10 ns pulse duration) pulse synchronized to probe the single particle on-the-fly as it traverses the optical cell. Some of the particle's fluorescence is collected by a reflective objective (NA 0.4, Newport 50105) and focused onto the slit of a spectrograph (Jobin Yvon, CP-140) for spectral dispersion. The fluorescence spectrum is recorded by the ICCD. The spectrometer slit width is set sufficiently large (1 mm) to allow fluorescence from particles throughout the sample volume to be collected by the highly (15 \times) magnifying reflective objective lens, but the wide slit reduces the spectral resolution to about 15 nm. A long-pass filter cutoff at 280 nm is used to block the elastic scattering from the 263 nm laser, but efficiently transmits the fluorescence with wavelength longer than 280 nm. The wavelength of the recording fluorescence spectra is determined by the elastic scattering peaks of the excitation laser with the first- and second-order scattering from the grating. The relative spectral response for the SPFS system is calibrated based on a NIST-traceable calibration light source from 220 to 1,050 nm (Ocean Optics, DH-2000-CAL deuterium tungsten halogen calibration standard).

Fluorescence spectra for single particles are obtained by subtracting an average of background spectra. The average background spectrum (for 100 shots) is recorded under the same experimental conditions, but without particles present in the optical cell by internally firing the laser at 10 Hz. The background counts of the ICCD are mainly from the elastic scattering, stray light, and the thermal and read-out noise of the ICCD.

3 Results and discussion

Figure 2 shows the measured particle size distributions of PM from the burn emissions of 12 sample materials. The particle count in the Y-axis is the averaged particle number per cm^3 per 100 s acquired during the entire burning process in the corresponding particle size interval. Each measurement took between about 10–30 min depending on the time required to heat the material and its burn rate. The burning generally started at furnace temperatures around 300–325 °C, except for the water bottle, which required a higher temperature of 420 °C (see Table 1). Some samples have the same label but are marked A, B, or C, which

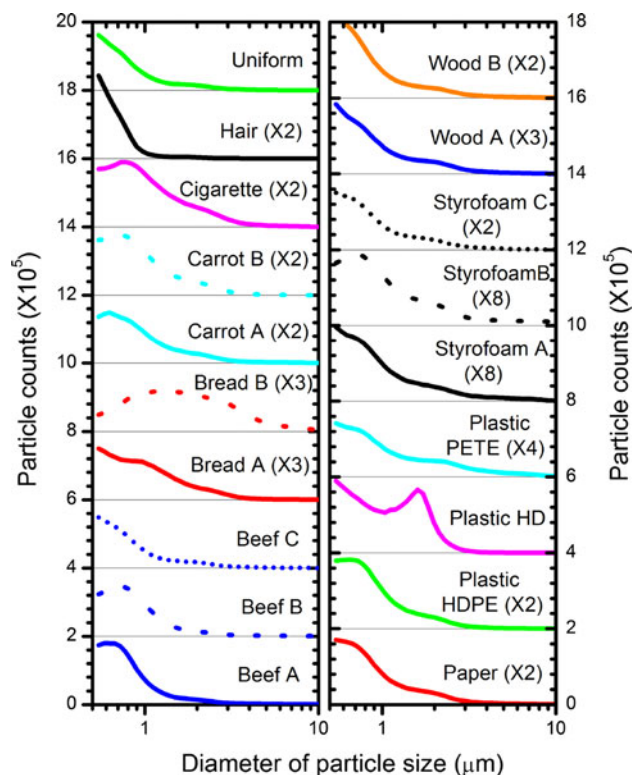


Fig. 2 Particle size distributions of the PM emissions from 12 burning materials measured by an aerodynamic particle sizer (TSI 3321). The burning temperature of the tube furnace was set between 290 and 420 °C for the different materials (see Table 1)

indicates chronologic progression of the burning stages when the UV-LIF spectra changed significantly throughout the burning process.

Figure 2 reveals the particle size from the emissions of the burning materials is dominated by small submicron particles with a small fraction in the 1–3 μm range. There are only tiny concentrations of particles above 3 μm , particularly for the emissions from burning human hair, which are nearly all smaller than 1 μm . However, the particle size is larger and is peaked around 2 μm for the plastic HD spoon and in the late burning stage for potato-roll bread. Most PM emissions appear to be dominated by submicron particles, consistent with previous observations of biomass burning [15, 16, 20, 21, 25]; so a scanning mobility particle sizer would be more suitable for obtaining better particle size distributions. However, the SPFS system as presently configured can only measure fluorescence of particles down to about 1 μm in diameter, so we emphasize supermicron particles here.

Long-duration exposure to high concentration particulate matter (PM) could cause health problems, and the smaller particles (PM 2.5, particles with a diameter of 2.5 μm and smaller) are considered to be more harmful than larger particles (PM10, particles with a diameter $\leq 10 \mu\text{m}$), regardless of the toxicity of materials that form the particles. Particles that are 10 μm or smaller generally pass through the throat, nose, and some enter the lungs. Once inhaled, these particles can affect the heart and lungs and can cause serious health effects [9]. Most of the particles from the emission of the 12 burning materials measured here have sizes predominately within the PM 2.5 range under the present burn conditions. This suggests that the particulate matter alone, apart from gases, could be harmful to the service members if exposed at high concentrations or for long duration.

During the burning process, all materials produce a large quantity of black smoke and gas. Visually it appears that significantly higher amounts of particulates are present at the beginning of a burn, as compared to the emissions produced during the stable combustion phase of the burn. Since there are very high concentrations of submicron particles drawn into the optical cell of the SPFS, for some trigger events multiple particles are in the illuminating beam of the SPFS. Consequently, some of the fluorescence spectra observed in these experiments are from multiple small particles, including some fluorescence emission generated from gases, within the sample volume of the SPFS (the sample volume is the intersection of the illuminating beam and the collection region of the SPFS reflective objective). Therefore, the fluorescence spectra we observed here are the combination of single-particle spectra and multiple particle spectra sensed during the burning process. We note that previous measurements of

atmospheric aerosol have only spectra of single particles [38].

During the burning process it is noteworthy that the general form of the fluorescence spectral profiles have only small variation for some materials (cigarette, hair, uniform, paper, and plastics), but change significantly for others (beef, bread, carrot, Styrofoam, and wood).

An example of small variability of spectral profiles during a burn process is found in Fig. 3, where typical single-laser-shot UV-LIF spectra and the corresponding contour map of the particulate emissions from burning plastic-PETE are shown. The 30 spectra presented were measured within a 10-min burn period, and were selected from thousands of recorded spectra with about 20 s separation between sequential spectra. Although there are large variations for the intensities and positions of various narrow peaks (mostly having widths $< 5 \text{ nm}$), the overall spectral profiles reveal only small changes during the entire burn process. The overall broad emission band covers 300–550 nm and peaks around 410 nm, although the absolute intensities of the spectra have significant variability.

An example of significant variability of fluorescence spectra of particulate emissions during a burn is for Styrofoam, as presented in Fig. 4. Again the 30 spectra (with corresponding contour map) were selected from 1,000 of recorded spectra with about 20 s separations between sequential spectra. In this case the overall spectral profiles evolve from a single band (peaking around 310 nm) gradually into two bands (peaking around 310 and 430 nm) when excited by a 263-nm laser. The 430-nm band begins with weak shoulder, becomes stronger, and eventually reaches intensity comparable to the 310 nm peak (see averaged spectra shown as Styrofoam C in Fig. 5).

In order to reveal how fluorescence spectral profiles evolve during the burning phases of various materials under study, we summarize the spectral data taken throughout the burns in Fig. 5. Presented are averaged (1,000 laser-shot) UV-LIF spectra of the particulate emissions from 12 burning materials (given in Table 1). If the fluorescence spectral profiles have only little change during the burn period, only one averaged UV-LIF spectrum is shown. If on the other hand, the fluorescence spectral profiles change significantly during the burn period, two or more averaged UV-LIF spectra are presented for that material.

In order to better quantify the spectral changes that evolve during a burn process, we calculated the intensity ratio of visible (400–560 nm)/ultraviolet (280–400 nm) fluorescence bands ($I_{\text{vis}}/I_{\text{UV}}$) for different burn phases of the various test materials. Table 2 summarizes the results. As noted above, some of the fluorescence spectral profiles exhibit only small variation during the burning process (for

Fig. 3 Landscape display of 30 typical UV-LIF spectra (and corresponding contour map) of the particulate emissions from burning plastic-PETE. The spectra were measured during an approximate 10 min burn period. The 30 spectra were selected from thousands of recorded spectra with about 20 s separation between sequential spectra. The spectral profiles display little variation during the entire burn process and have a single broad fluorescence emission band from 300 to 550 nm peaking around 410 nm (excited by a 263 nm laser)

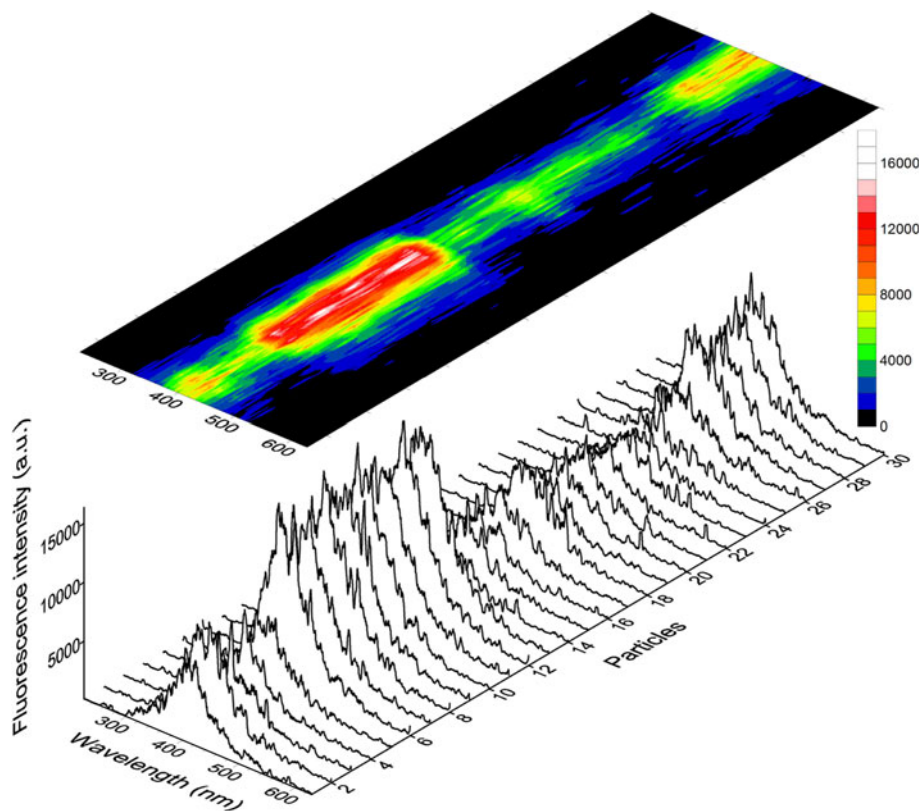
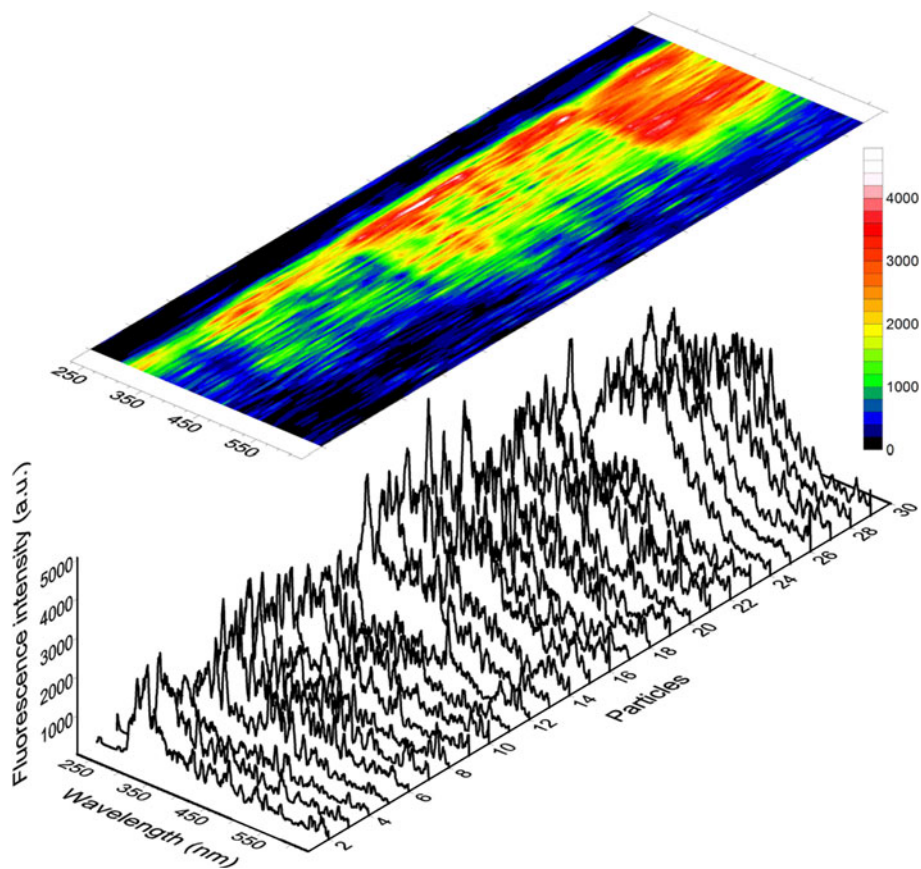


Fig. 4 Thirty typical single-particle UV-LIF spectra (as in Fig. 3) except for emissions from burning Styrofoam. The overall spectral profiles change from a single band (peaked around 300 nm) gradually into two bands (peaked around 310 and 430 nm)



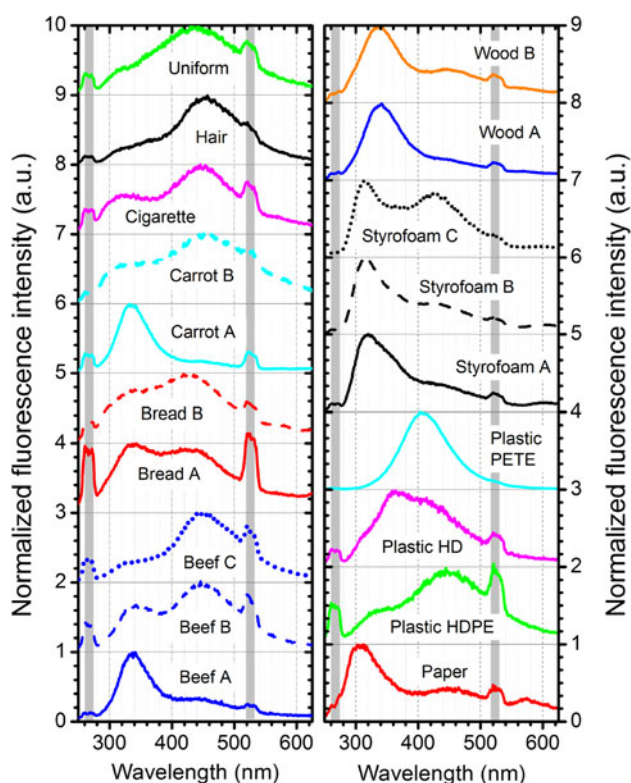


Fig. 5 Average (1,000 laser-shot) UV-LIF spectra of particulate emissions from various burning materials. The 263 nm peaks are the leaking elastic scattering from the laser, and the 527 nm peaks are from the second order of the grating. If the fluorescence spectral profiles undergo only small changes during the burn process (as for the battle-dress uniform, human hair, cigarette, plastic water bottle, plastic spoon, plastic cup, and shredded white paper samples), only one average UV-LIF spectrum is shown. If the fluorescence spectral profiles change significantly during the burn process (as for shredded carrots, potato-roll bread, cooked hamburger meat, wood shards, and styrofoam cup), two or more average UV-LIF spectra are presented

cigarette, hair, uniform, paper, and plastics), and the ratio ($I_{\text{vis}}/I_{\text{UV}}$) changes by at most 10 %. On the other hand, the fluorescence spectra of other materials (beef, bread, carrot, Styrofoam, and wood) evolve from a single UV peak (around 310–340 nm) into a bimodal spectrum with another visible peak (around 430–450 nm) during the burn process. The corresponding fluorescence intensity ratio ($I_{\text{vis}}/I_{\text{UV}}$) for these materials can be as much as a factor 10 (e.g., beef, carrot).

It is well known that many different materials are generated from burning processes, including soot (primarily composed of black carbon) and various organic carbon chemicals. The concentrations of different chemicals vary with burn conditions, burn phase, and materials burned [9, 19–27].

Polycyclic aromatic hydrocarbons are ubiquitous in emissions from open burns. With UV laser excitation, the fluorescence spectra of PAHs peak from 410 to 460 nm [27, 30]; water-dissolved PAHs have peaks from 300 to

460 nm with a broad band covering 300–600 nm [32–34]. Among the PAHs are compounds having a single aromatic ring such as tyrosine, but with different or additional conjugated bonds. Tyrosine-like chemicals (or TYLIS including benzoic acids, phenols, and benzaldehydes [32–34]) generally fluoresce around 310 nm. PAHs having double aromatic rings, such as tryptophan but with different or additional conjugated bonds (tryptophan-like or TRYLIS, including dibenzoic acids; naphthalene and its derivatives [32–34]) generally fluoresce around 320–340 nm. PAHs with heavier molecular weights (humic-like substances or HULIS, [32–34]) fluoresce further to the red, peaking from 400 to 460 nm (or even further) via 263 nm excitation. The fluorescence profiles from the 12 sample materials burned here reveal that there are likely some TYLIS, TRYLIS, and HULIS substances in the emissions from the burns, and probably more HULIS in the late stages of the burn process (see Table 2; Fig. 5).

It is interesting to compare the UV-LIF spectra of particulate emissions from burning materials to those observed from atmospheric aerosol particles. Previous analyses have shown that the fluorescence spectra of atmospheric aerosol particles at several sites in the US (Adelphi MD, New Haven CT, and Las Cruces NM) can be grouped into 8–10 clusters [37, 38, 40]. These clusters are determined by hierarchical clustering analysis from millions of single-particle spectra measured at the three sites. The results showed that particles with spectra that are clustered into the 10 templates occupied more than 90 % of the whole fluorescent particles, and the un-clustered particles cannot be grouped into any template that has a population higher than 1 %. A comparison of the fluorescence spectra of the particulate emissions from the burns to four of the atmospheric aerosol spectral clusters is presented in Fig. 6.

It is evident that about 68 % fluorescence spectra of the burn emissions of the 12 sample materials are similar to atmospheric aerosol clusters labeled 2, 3, 5 and 8. Some are very similar such as carrot A to cluster 2, beef A to cluster 3, and plastic HDPE to cluster 8. Some are only vaguely similar such as wood B to cluster 3, plastic HD to cluster 5, cigarette and hair to cluster 8. This suggests that some atmospheric aerosol may derive from burning of biomass (and possibly garbage) in the atmosphere. On the other hand, some fluorescence spectra of burn emissions do not match any spectra of atmospheric aerosol clusters such as beef B, bread A, and Styrofoam C, which all have bimodal fluorescence peaks. The reason may be that aging of some chemicals in burn emissions might occur quickly during transport and diffusion processes in the atmosphere. If this is true, distinctly bimodal fluorescence peaks within atmospheric aerosol particles could be evidence for their source being close to an atmospheric burn of biomass, garbage, or other waste material. The fluorescence spectral

Table 2 Listed are major peaks of the fluorescence spectra of emissions from burning materials (263 nm excitation)

Material	Beef	Bread	Carrot	Cigarette	Hair	Uniform
Fluor. peaks (nm)	340, 450	330, 430	330, 450	320, 450	320, 450	320, 440
Overall profile change (I_{vis}/I_{UV})	Large (0.30 → 3.42)	Large (0.89 → 1.41)	Large (0.21 → 2.03)	Small (0.53 → 0.59)	Small (4.40 → 4.46)	Small (2.38 → 2.52)
Percentage of burn particle spectra falling into previously found atmospheric aerosol clusters	A:89 % cluster 3 B: no fitting C:37 % cluster 8	A:no fitting B:74 % cluster 8	A:92 % cluster 2 B:75 % cluster 8	21 % cluster 8	27 % cluster 8	72 % cluster 8
Material	Paper	Plastic HDPE	Plastic HD	Plastic-PETE	Styrofoam	Wood
Fluor. peaks (nm)	310, 450	330, 440	360, 430	410	310, 430	340, 440
Overall profile change (I_{vis}/I_{UV})	Small (0.42 → 0.44)	Small (2.08 → 2.26)	Small (0.78 → 0.82)	Small (one peak)	Large (0.34 → 0.88)	Large (0.29 → 0.52)
Percentage of burn particle spectra falling into previously found atmospheric aerosol clusters	35 % cluster 1	83 % cluster 8	51 % cluster 5	No fitting	A:76 % cluster 2 B:61 % cluster 2 C:no fitting	A:90 % cluster 3 B:85 % cluster 3

Also given are the ratios of the corresponding visible peak to the UV peak ($I_{vis}(400\text{--}560\text{ nm})/I_{UV}(280\text{--}400\text{ nm})$) of fluorescence spectra observed during the burn process, and the percentage of fluorescent spectra that fall into previously found spectral clusters of fluorescent atmospheric aerosol particles

profiles from burning materials detected here are even easier to be discriminated from the time-integrated fluorescence spectral profiles [41, 42], which are obtained from the UV-LIF spectra of a group of atmospheric particles from thousands to a few tens of thousands detected very 10 min in three different locations. This implies that SFFS system might be a good tool for monitoring burning pit emission via fluorescence spectral profile discrimination.

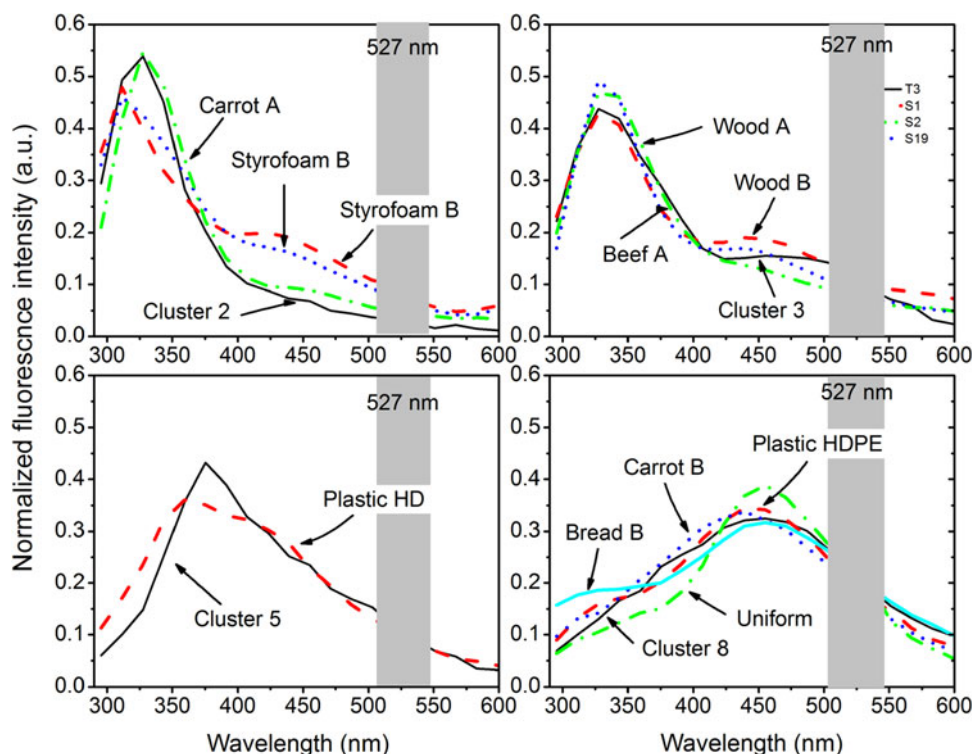
Data in Table 2 reveal the percentages of single shot fluorescence spectra of burn particulate emissions that are similar to the cluster spectra of atmospheric aerosol particles. Total about 68 % of the spectra from the various burn emissions are similar to atmospheric aerosol clusters labeled 2, 3 and 8. Clusters 2 and 3 are similar to the spectra from bacteria, while cluster 8 is similar to the spectra from humic/fulvic acids, humic-like substances, and combinations of PAHs [37, 38, 40]. However, it is still hard, at the present stage, to speculate on the contribution of burn particulate emissions to atmospheric aerosol from these data.

Regarding possible health effects of burn emissions, Lemieux et al. [23] summarize the emissions of organic air toxins from open burning and PAHs are believed to be important for health problems. The potential cancer risk associated with PAH exposure through inhalation can be estimated based on the benzo[a]pyrene toxic equivalence (BaPeq), where the overall toxicity of a PAH mixture is defined by the concentration of each compound multiplied by its relative toxic equivalence factor (TEF) [19]. Here, we would not be able to determine the overall toxicity or identifications of chemicals from the burning process with the limited information available from fluorescence spectra measurements alone. However, the evolution of the overall spectral profiles for different materials during burning process could supply some information for understanding the toxicity of burning emissions, as well as supply a possible monitoring tool. Further systematic and controlling study is required for better understanding of the application with single-particle fluorescence spectra technology in burn pit monitoring.

4 Summary

A single-particle ultra-violet laser-induced fluorescence spectrometer (SPFS) and an aerodynamic particle sizer were used to measure the fluorescence spectra and particle size distribution from the particulate emissions of 12 different burning materials burned in a tube furnace to simulate open-air burning of garbage. The particles in the emissions are dominated by particles $<1\ \mu\text{m}$ in diameter, and with a small fraction in the 1–3 μm range which were measured here. There are small changes in the fluorescence

Fig. 6 Comparison of some averaged fluorescence spectral profiles from the emission of burning samples with the clustered fluorescence template spectra from atmospheric aerosol measurements [40]



spectral profiles for some materials during the burning process (cigarette, hair, uniform, paper, and plastics); but large changes for the others (beef, bread, carrot, Styrofoam, and wood). The spectral profiles for beef, bread, carrot, Styrofoam, and wood gradually evolved from spectra having a single UV peak (around 310–340 nm) into bimodal spectra with another visible peak (around 430–450 nm) with increasing intensity during the burn. The SPFS technology could possibly be used to monitor and help classify particulate emissions from open-air burn pits.

Acknowledgments This research was supported by the US Army Research Laboratory mission funds and encouraged by the US Army Public Health Command.

Open Access This article is distributed under the terms of the Creative Commons Attribution License which permits any use, distribution, and reproduction in any medium, provided the original author(s) and the source are credited.

References

1. K. Kennedy, Burn Pit at Balad Raises Health Concerns. *Army News*, 2008, http://www.armytimes.com/news/2008/10/military_burnpit_102708w/
2. A. Levine, Gulf War Syndrome-VA to Look into Effects of 'Burn Pits' on Veterans, *CNN US*, 2009, http://articles.cnn.com/2009-03-17/us/burn.pits_1_pits-exposures-gulf-war-syndrome?_s=PM:US
3. J. Risen, Veterans Sound Alarm Over Burn-pit Exposure. *The New York Times*, 2010, <http://www.nytimes.com/2010/08/07/us/07burn.html>
4. R. F. DeFraites, Epidemiological Studies of Health Outcomes among Troops Deployed to Burn Pit Sites, 2010, http://www.afhsc.mil/viewDocument?file=100604_FINAL_Burn_Pit_Epi_Studies.pdf
5. Long-Term Health Consequences of Exposure to Burn Pits in Iraq and Afghanistan. *Institute of Medicine*, 2011, http://books.nap.edu/openbook.php?record_id=13209
6. The Air over There: ARL's Battlefield Environment Experts' Collection of Risky, Tiny Particles Could Solve Future Mysteries in Soldier Medicine. *US Army Research Laboratory News*. 2011, <http://www.arl.army.mil/www/default.cfm?page=642>
7. B. Smith, C.A. Wong, E.J. Boyko, C.J. Phillips, J.D. Gackstetter et al., The effects of exposure to documented open-air burn pits on respiratory health among deployers of the millennium cohort study. *J. Occup. Environ. Med.* **54**(6), 708–716 (2012)
8. M.S. King, R. Eisenberg, J.H. Newman, J.J. Tolle, F.E. Harrell et al., Constrictive bronchiolitis in soldiers returning from Iraq and Afghanistan. *N. Engl. J. Med.* **365**, 222–230 (2011)
9. Environmental Hazards in Iraq, Afghanistan, and Other Military Installations. *Military Community*, 2010, <http://forums.military.com/eve/forums/a/tpc/f/8280047191001/m/9740039052001>
10. Burn Pits, *Public Health, US Department of Veterans Affairs*, 2012, <http://www.publichealth.va.gov/exposures/burnpits/index.asp>
11. S.S. Leonard, S.W. Wang, X.L. Shi, B.S. Jordan, V. Castranova et al., Wood smoke particles generate free radicals and cause lipid peroxidation, DNA damage, NF kappa B activation, and TNF-alpha release in macrophages. *Toxicology* **150**(1–3), 147–157 (2000)
12. C.A. Pope, R.T. Burnett, M.J. Thun, E.E. Calle, D. Krewski et al., Lung cancer, cardiopulmonary mortality, and long-term exposure to fine particulate air pollution. *J. Am. Med. Assoc.* **287**, 1132–1141 (2002)
13. P.H. Danielsen, S. Loft, A. Kocbach, P.E. Schwarze, P. Møller, Oxidative damage to DNA and repair induced by norwegian wood smoke particles in human A549 and THP-1 cell lines. *Mut. Res. Gen. Toxicol. Environ. Mut.* **674**(1–2), 116–122 (2009)

14. J.S. Reid, T.F. Eck, S.A. Christopher, R. Koppmann, O. Dubovik et al., A review of biomass burning emissions part III: intensive optical properties of biomass burning particles. *Atmos. Chem. Phys.* **5**, 827–849 (2005)
15. R.K. Chakrabarty, H. Moosmüller, W.P. Arnott, M.A. Garro, J.G. Slowik et al., Light scattering and absorption by fractal-like carbonaceous chain aggregates: comparison of theories and experiment. *Appl. Opt.* **46**(28), 6990–7006 (2007)
16. B. Miljevic, M.F. Heringa, A. Keller, N.K. Meyer, J. Good et al., Oxidative potential of logwood and pellet burning particles assessed by a novel profluorescent nitroxide probe. *Environ. Sci. Technol.* **44**, 6601–6607 (2010)
17. D. Xanatflores-Cervantes, C.M. Reddy, P.M. Gschwend, Inferring black carbon concentrations in particulate organic matter by observing pyrene fluorescence losses. *Environ. Sci. Technol.* **43**, 4864–4870 (2009)
18. G.A. Rechtsteiner, C. Felix, A.K. Ott, O. Hampe, R.P. Van Duyn et al., Raman and fluorescence spectra of size-selected, matrix-isolated C14 and C18 neutral carbon clusters. *J. Phys. Chem. A* **105**, 3029–3033 (2001)
19. F.S. Silva, J. Cristale, P.A. André, P.H.N. Saldiva, M.R.R. Marchi, PM2.5 and PM10: the influence of sugarcane burning on potential cancer risk. *Atmos. Environ.* **44**, 5133–5138 (2010)
20. L.L. Soto-Garcia, M.O. Andreae, T.W. Andreae, P. Artaxo, W. Maenhaut et al., Evaluation of the carbon content of aerosols from the burning of biomass in the Brazilian Amazon using thermal, optical and thermal-optical analysis methods. *Atmos. Chem. Phys.* **11**, 4425–4444 (2011)
21. E.J.T. Levin, G.R. McMeeking, C.M. Carrico, L.E. Mack, S.M. Kreidenweis et al., Biomass burning smoke aerosol properties measured during Fire Laboratory at Missoula Experiments (FLAME). *J. Geophys. Res.* **115**, D18210 (2010)
22. R.K. Chakrabarty, H. Moosmüller, M.A. Garro, W.P. Arnott, J. Walker et al., Emissions from the laboratory combustion of wildland fuels: particle morphology and size. *J. Geophys. Res.* **111**, D07204 (2006)
23. P.M. Lemieux, C.C. Lutesb, D.A. Santoianni, Emissions of organic air toxics from open burning: a comprehensive review. *Prog. Energy Combust. Sci.* **30**, 1–32 (2004)
24. K.A. Pratt, A.J. Heymsfield, C.H. Twohy, S.M. Murphy, P.J. Demott et al., In situ chemical characterization of aged biomass-burning aerosols impacting cold wave clouds. *J. Atmos. Sci.* **67**, 2451–2468 (2010)
25. M.D. Hays, C.D. Geron, K.J. Linna, N.D. Smith, J.J. Schauer, Speciation of gas-phase and fine particle emissions from burning of foliar fuels. *Environ. Sci. Technol.* **36**(11), 2281–2295 (2002)
26. G.R. McMeeking, S.M. Kreidenweis, S. Baker, C.M. Carrico, C. Chow et al., Emissions of trace gases and aerosols during the open combustion of biomass in the laboratory. *J. Geophys. Res.* **114**, D19210 (2009)
27. S.A. Bortolato, J.A. Arancibia, G.M. Escandar, Chemometrics-assisted excitation-emission fluorescence spectroscopy on nylon membranes. Simultaneous determination of benzo[a]pyrene and dibenz[a, h]anthracene at parts-per-trillion levels in the presence of the remaining EPA PAH priority pollutants as interferences. *Anal. Chem.* **80**, 8276–8286 (2008)
28. T. Pagano, A.D. Ross, J. Chiarellib, J.E. Kenny, Multidimensional fluorescence studies of the phenolic content of dissolved organic carbon in humic substances. *J. Environ. Monit.* **14**, 937–943 (2012)
29. M.S. Johnson, E.G. Couto, M. Abdo, J. Lehmann, Fluorescence index as an indicator of dissolved organic carbon quality in hydrologic flowpaths of forested tropical watersheds. *Biogeochemistry* **105**, 149–157 (2011)
30. E.-J. Ko, K.-W. Kim, U. Wachsmuth, Remediation process monitoring of PAH-contaminated soils using laser-induced fluorescence. *Environ. Monit. Assess.* **92**, 179–191 (2004)
31. P.A. Lieberzeit, K. Halikias, A. Afzal, F.L. Dickert, Polymers imprinted with PAH mixtures—comparing fluorescence and QCM sensors. *Anal. Bioanal. Chem.* **392**, 1405–1410 (2008)
32. P.G. Coble, Characterization of marine and terrestrial DOM in seawater using excitation-emission matrix spectroscopy. *Mar. Chem.* **51**, 325–346 (1996)
33. P. Kowalczyk, W.J. Cooper, M.J. Durako, A.E. Kahn, M. Gonsior et al., Characterization of dissolved organic matter fluorescence in the South Atlantic Bight with use of PARAFAC model: relationships between fluorescence and its components, absorption coefficients and organic carbon concentrations. *Mar. Chem.* **118**, 22–36 (2010)
34. C.L. Muller, A. Baker, R. Hutchinson, I.J. Fairchild, C. Kidd, Analysis of rainwater dissolved organic carbon compounds using fluorescence spectrophotometry. *Atmos. Environ.* **42**, 8036–8045 (2008)
35. F. Lewitzka, R. Niessner, Application of time-resolved fluorescence spectroscopy on the analysis of PAH-coated aerosols. *Aerosol Sci. Technol.* **23**(3), 454–464 (2007)
36. Y.L. Pan, J. Hartings, R.G. Pinnick, S.C. Hill, J. Halverson et al., Single-particle fluorescence spectrometer for ambient aerosols. *Aerosol Sci. Technol.* **37**, 628–639 (2003)
37. R.G. Pinnick, S.C. Hill, Y.L. Pan, R.K. Chang, Fluorescence spectra of atmospheric aerosol at Adelphi, Maryland, USA: measurement and classification of single particles containing organic carbon. *Atmos. Environ.* **38**, 1657–1672 (2004)
38. Y.L. Pan, R.G. Pinnick, S.C. Hill, R.K. Chang, Particle-fluorescence spectrometer for real-time single-particle measurements of atmospheric organic carbon and biological aerosol. *Environ. Sci. Technol.* **43**, 429–434 (2009)
39. R. DeFreez, LIF bio-aerosol threat triggers: then and now. *Proc. SPIE* **7484**, 74840H 2009 (pp 15)
40. Y.L. Pan, R.G. Pinnick, S.C. Hill, J.M. Rosen, R.K. Chang, Single-particle laser-induced-fluorescence spectra of biological and other organic-carbon aerosols in the atmosphere: measurements at New Haven, CT and Las Cruces, NM, USA. *J. Geophys. Res.* **112**, D24S19 (2007)
41. Y.L. Pan, H. Huang, R.K. Chang, Clustered and integrated fluorescence spectra from single atmospheric aerosol particles excited by a 263- and 351-nm laser at New Haven, CT, and Adelphi, MD. *J. Quant. Spectrosc. Radiat. Trans.* **113**, 2213–2221 (2012)
42. R.G. Pinnick, E. Fernandez, J.M. Rosen, S.C. Hill, Y. Wang, Y.L. Pan, Fluorescence spectra and elastic scattering characteristics of atmospheric aerosol in Las Cruces, New Mexico, USA: variability of concentrations and possible constituents and sources of particles in various spectral clusters. *Atmos. Environ.* **65**, 195–204 (2013)